DOI: 10.13009/EUCASS2025-016
11TH EUROPEAN CONFERENCE FOR AERONAUTICS AND SPACE SCIENCES (EUCASS)

Optimization of Hydrogen Semi-BWB type Airliner based on International Air-route Market Performance

Jaesan Yoon
Korea Aerospace Industries, NACS Team
Sacheon-si, 52529, Gyeongsangnam-do, Republic of Korea – jaesan.yoon1@koreaaero.com, jae0204@gmail.com

Abstract
Reducing emission from airliners is one of important issue for the green-aviation. Hydrogen fuelled aircraft is one of the future candidates which contributes the emission reduction, however the thermal and mechanical characteristics of the hydrogen require very different configuration to achieve given range performance goal. Author organizes sizing process including prediction of weight, fuel volume, aerodynamic characteristics and its performance based on the parametric controlled external configuration. Performance and fuel efficiency of the configuration is evaluated in the international air-route network, and the configuration is optimized for operation efficiency of the possible airlines.

Nomenclature

BWB	Blended Wing Body
LH2	Liquid Hydrogen
O&S	Operation and Support
SOFC	Solid Oxide Fuel Cell
TSFC	Thrust Specific Fuel Consumption [lb/lbf/h]
AoA	Angle of attack
cts	unit of drag coefficient (0.0001)
$C_{L,D}$	Lift, Drag Coefficient
L/D	Lift-to-Drag ratio
M_{crit}	drag-diverged critical Mach number
t/c	wing thickness-to-chord ratio
T/W	Thrust-to-Weight ratio
W/S	Wing loading (Weight-to-Wing-Area) [lb/ft^2]
θ	Wing Root Sweep Angle

1. Introduction

A revenue passenger mile (RPM) has been increased since dawn of civil aviation, and its incomparable speed makes itself irreplaceable. Although the efficiency of the airliners improved, total emissions from the aviation sector is hard to be decreased due to its increasing popularity. Using hydrogen as energy source instead of hydrocarbon based fuel is one of the future aviation option that reduces greenhouse gas emission [1]. Both direct combustion and fuel-cell are considered, and the technical demonstration for scalability of propulsion system is in progress [2, 3]. LH2 fuel tanks have different characteristics compare to the hydrocarbon ones, low mass density of fuel, requiring heat insulation, and high heat per unit mass. These prevents usage of wet-wing-tank, and leads to volumetric and ellipsoidal shape for the LH2 tanks. For the short range, level of regional jet or single aisle airliner, small ellipsoidal tank or additional pod shape attached inside or outside of the aircraft is acceptable however, massive size of the LH2 tank for the long-haul airliners requires radical change of the configuration.

Indeed, new configurations rather than conventional tube-and-wing airliner have been proposed to carry LH2 fuel, passenger, and cargo effectively. Blended wing body (BWB) has been proposed [3, 4] to accommodate huge volume of LH2 tank with better aerodynamic efficiency. Studies for the BWB is very promising, and JetZero [5] is forehead of application that they currently build full scale technical demonstrator. Instead, BWB made their step; this configuration should overcome many aspect of hurdles from design, safety, manufacturing, verification, and

DOI: 10.13009/EUCASS2025-016

certification. Author proposed Semi-BWB [6] configuration that retain conventional fuselage, vertical tail and horizontal tail compared to the BWB. This configuration is still familiar to the most of the airliner manufacturer and engineers while it could keep large LH2 tank on its wing root replacing thin-wet-wing fuel tank. If the semi-BWB is applied to the LH2 long-haul airliners, the new sizing result, estimated weight, passenger capacity, and overall geometry, is required because of very different gravimetric, volumetric characteristics of the new fuels. This sizing result would be future guidance value for the system engineers working on the future LH2 aviation.

This paper provides sizing and configuration framework for LH2 semi-BWB airliner; author optimizes the configuration based on the operation effectiveness and market competitiveness. Parametric configuration builds estimated aerodynamic, weight, fuel tank volume, weight, and number of passenger of the airliner. The air-route of international major cities generates market environment that the airliner would be operated; earning of the airline is function of number of passenger, fuel usage, and maximum range. Study range of configuration parameter is given, and database relation among configuration, performance, and operation effectiveness is generated via Monte Carlo method. Generic, and NLPQLP algorithm is used to optimize configuration to meet the best market earning of operating airline. This overall progress described above is summarized in Fig. 1.

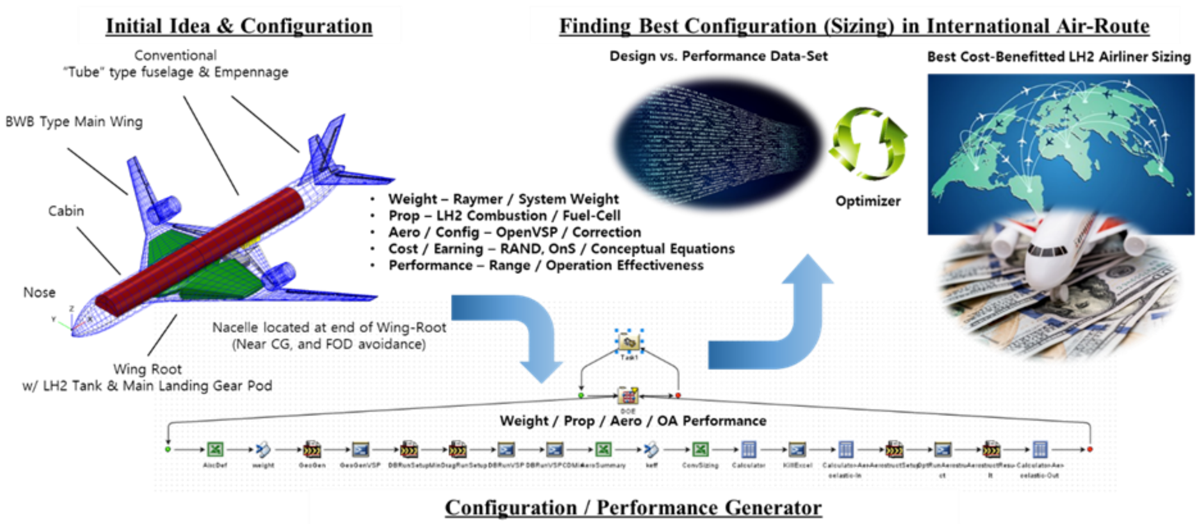

Figure 1: Overall framework of design and optimization process for Semi-BWB LH2 long-haul airliner

2. Methodology

2.1 Aircraft configuration and sizing methodology

The baseline configuration of Semi-BWB LH2 long-haul airliner is a twin-aisle fuselage with BWB type wing while conventional vertical and horizontal tail are at the empennage. Hydrogen combustion engines and their nacelles are located at the trailing edge of wing root where three LH2 tank is installed to maximize volume-to-surface ratio of extremely cold LH2 as shown in Fig. 2. As described in Author's previous research [6], it could avoid FOD (Foreign Object Damage), heat dissipation of LH2 fuel tank, BWB's sensitive stability and control issue, and has advantage in derivatives development due to the conventional stabilizers, near-CG-layout of major components, and high position of engines. Compare to the previous research for the military transport, maximum height of the wing root is lower than that of cabin because emergency exit doors should be secured for passengers. Volume for passenger cabin is upper half of tube type fuselage contrary to that of military one having all cylindrical cargo volume which only allow fuel tank in its wing root. Undercarriage is expected to be located at behind of the LH2 tanks, and Hybrid fuel cell is at behind of them if designer decide to use it as power generator.

Aircraft configuration is parameterized to investigate its optimum; some of them are independent input while others are determined from the independent ones. The other dependents are geometry of stabilizer and position of nacelle calculated by the independent inputs like wing area, span and stream-wise position of wing root. Few parameters, length of nose, tail, dihedral angle of horizontal stabilizer, and size of nacelles are fixed and expected to have insignificant impact than the selected design parameters as shown in Fig. 3. The parametric configuration is generated by OpenVSP script, and dependent parameters like fuel tank volume, number of passengers on board, are also

DOI: 10.13009/EUCASS2025-016

automatically determined by geometry. Whole list of independent, dependent, and constant design parameters is shown in Table 1; remained configuration parameters and other input parameters like correction factor for Raymer's weight prediction [7], propulsion, air-route, and cost factors are also listed.

Weight prediction of the LH2 aircraft can be a controversial issue because, unlike conventional jet fuel, LH2 requires heat insulated structure and related support system. This paper follows trends of references [8, 9], and adds LH2 induced weight based on the Raymer's [7] components estimation equation; 10% of fuel weight for fuel system, replacing original fuel system weight prediction, and 31.6% of fuel weight are added to consider them. Other terms follow Raymer's relation among fuel weight, payload, empty weight, and maximum takeoff weight of jet transport without modification, then initial guessing value is re-distributed to the equation of components to finalize the estimation. Initial payload and fuel weight is proportional to the cabin and fuel tank volume, respectively. This model assumes that the cabin size and following payload weight of baseline are same as that of 787 class airliner, 53t. If fuselage length and width is changed, payload weight is proportionally followed product of length and width. As described above, three LH2 fuel tanks are located inside of wing root and fuselage, and total volume of them are calculated from the ellipsoidal shape. Their size and position is function of chord, width, span of fuselage and wing root part. Based on reference [9], 92.7% of volume is useful for LH2, and remained 7.3% is for baffle, integrated structure, and heat insulation materials for the case of integrated LH2 tank-structure.

LH2 based propulsion system can be divided to two options; the first one is hydrogen combustion engines while the second one is fuel cell powered system. Weight and size factor of propulsion system is firstly given as TSFC; the value is estimated from hydrocarbon fuelled high-bypass turbofan engine. Generally, state-of-art TSFC of the hydrocarbon fuelled engine at sea level is 0.41 lb/lbf/h and it is increased about 1.5 times at 35kft cruise altitude. This is proportionally decreased via heat value per unit mass of hydrogen and hydro-carbon fuel, and as a result, author uses little bit conservative value as 0.25 lb/lbf/h at 35kft altitude. Sizing and weight specification of fuel cell power pack is following work of Patel et al. [10]; specific power per weight is given for fuel-cell-stack, motor-thermal-management, fan-drive, high-temperature super-conducting (HTS) generator, and fuel-cell cooling components. As the hybridization of overall power, required fuel-cell generated power, is given, additional weight can be calculated from it. Generally, fuel-cell, assumed as solid oxide fuel cells (SOFC) here, is more efficient than gas combustion one for about 50%, instead, it has heavier weight. TSFC of current fuel cell model with efficiency loss of the system components is about 0.149 lb/lbf/h. Scalability issue of the SOFC for the long-haul airliner would not be discussed here.

VSPAero estimates lift and induced drag characteristics in cruise Mach condition while skin-friction drag term is given by VSPAero's empirical formula. Author adds Korn's wave drag equation as shown in Eq. (1) to predict drag-diverged critical Mach number (M_{crit}), and adds amount of transonic drag rise ($C_{D\ Rise}$) if excessive wing thickness and smaller swept angle were applied. More than that, 5cts of additional drag is applied for miscellaneous parts which is not described in OpenVSP. Although semi-BWB has very thick airfoil around root reducing M_{crit}, small wing loading, leading smaller $C_{L\ cruise}$, and higher swept angle at root make similar M_{crit} that of the conventional high subsonic airliners. Tessellation numbers for vortices-lattice method (VLM) is shown in Fig. 4 which number is unchanged during the sizing studies. Overlapped part of wing and fuselage is regarded as elliptical shape to describe the fuselage fairing.

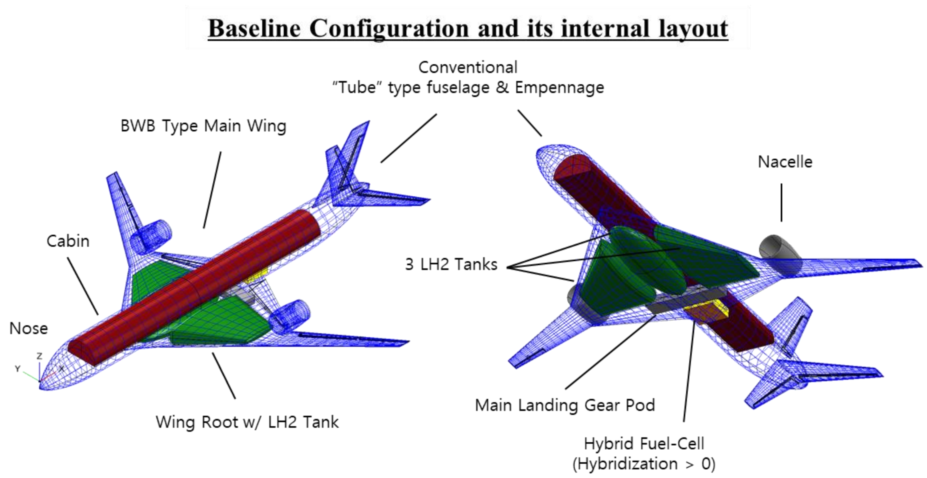

Figure 2: Baseline configuration of the LH2 Semi-BWB long range airliner and internal layout of major components

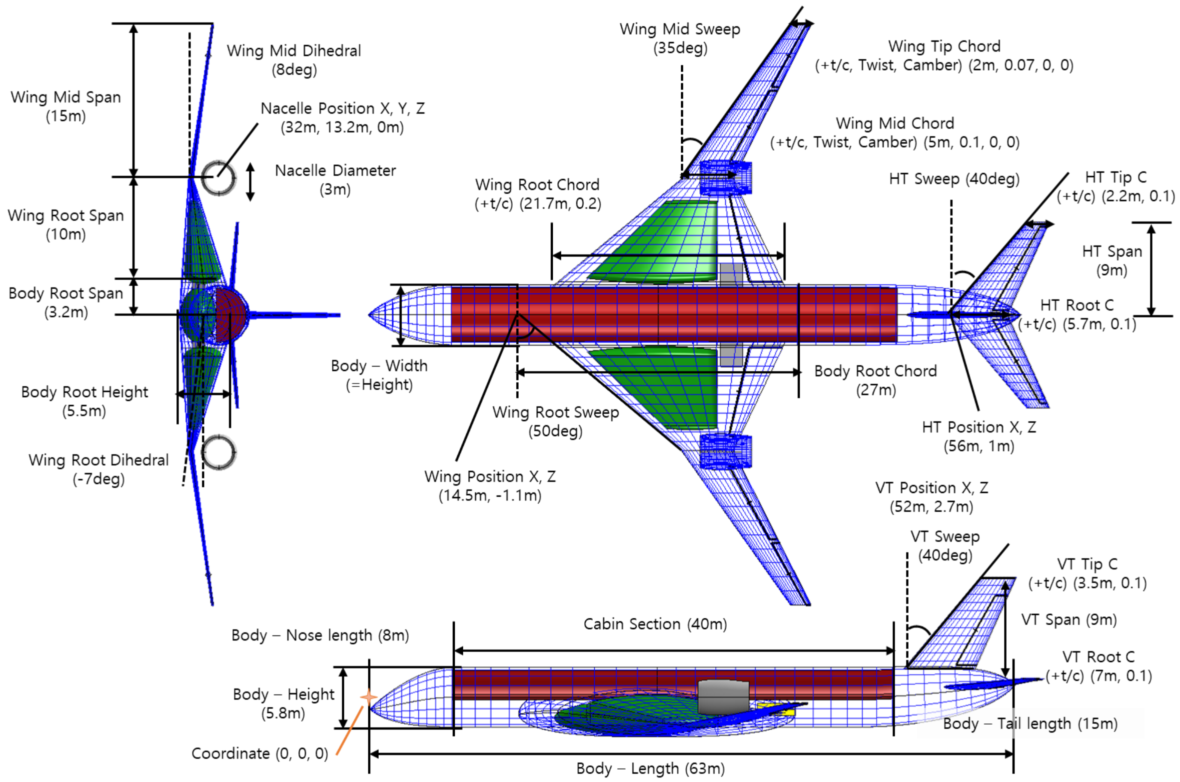

Figure 3: Design parameters and their values for the baseline

Table 1: List of design parameters and their sizing specifications

Components	Parameter	Baseline	Principle	Study Range / Equation
Body	Length, Width	63, 5.8	Study Parameter	45 ~ 80, 4.5 ~ 7.5 (Size from B767 to A380)
	Height	5.8	Dependents	= Body.Width
	Nose section Ratio (pos.)	0.127 (8)	Fixed	Fixed length
	Tail section Ratio (pos.)	0.762 (48)	”	“
Body Root	Height	5.5	Dependents	= Body.Width - 0.3
	Chord	27	Study Parameter	20 ~ 45
	Span	3.2	Dependents	= BodyWidth/2 + 0.3
	Wing Pos. (X, Z)	14.5, -1.1	”	= Body Mid Position – BodyRootChord$_{study}$/2, = 1.8 - Body.Height/2
Nacelle	Pos. (X, Y, Z)	32, 13.2, 0	”	At Wing Root End f’n
	Diameter	3	Fixed	
HT	Sweep [deg]	40	Dependents	= Wing.Mid.Sweep + 5

DOI: 10.13009/EUCASS2025-016

	Root C, Tip C, Span	5.7, 2.2, 9	”	= Baseline va;ie $(WingA_{study}/WingA_{Baseline})^{0.5}$
	Root t/c, Tip t/c	0.1, 0.1	Fixed	
	Pos. (X, Z)	56, 1	Dependents	At the empennage f’n
VT	Sweep [deg]	40	”	= Wing.Mid.Sweep + 5
	Root C, Tip C, Span	7, 3.5, 9	”	Baseline value $(WingArea_{new}/WingArea_{Baseline})^{0.5}$
	Root t/c, Tip t/c	0.1, 0.1	Fixed	
	Pos. (X, Z)	52, 2.7	”	At the empennage f’n

Components	Parameter	Baseline	Principle	Study Range / Equation
Wing Root	Sweep [deg]	50	Study Parameter	35 ~ 55
	Chord	27	”	20 ~ 45
	t/c	0.2	Dependents	= RootHeight / RootTipC*0.2/0.254
	Span	10	Study Parameter	4 ~ 9
	Dihedral [deg]	-7	”	-10 ~ -2
Wing Mid/Tip	Sweep [deg]	35	”	35 ~ 55
	Mid C [m]	5	”	4 ~ 15
	Mid Span	15	”	7 ~ 30
	Mid Dihedral	8	”	3 ~ 12
	Mid t/c	0.1	”	0.08 ~ 0.14
	Tip C [m]	2	”	1.5 ~ 3
	Tip t/c	0.07	”	0.04 ~ 0.1
	Mid Twist [deg]	0	”	-3 ~ 4
	Tip Twist [deg]	0	”	-5 ~ 3
	Mid Camber [C_L]	0	”	-0.2 ~ 0.6
	Tip Camber [C_L]	0	”	0 ~ 0.5

Components	Parameter	Baseline	Principle	Study Range / Equation
Weight	Correction Factor	1.0	Study Parameter	0.9 ~ 1.1
Propulsion	TSFC [lb/lbf/h]	0.25	”	0.2 ~ 0.3
	Thrust [lbf]	50,000	”	400 ~ 150,000
	Hybridization	0	”	0 ~ 0.4

DOI: 10.13009/EUCASS2025-016

	Fuel Cell Efficiency	0.55	”	0.3 ~ 0.6
Route / Earning	Pax [#]	290	Dependents	290 * (Cabin_Area_new/Cabin_Area_ref)
	Route Num. [#]	197	Calculated From City list (See Table 2)	If Dist. < 400nm, Excluded If flight hr < 4hr, Twice per day
	Route Popularity	See Table. 2		= Product of popularity of connected cities
	Earning Per 1# Route	963.3		= Route Popularity * (NumPax*NumTrip) ^ PaxFactor * City Distance
Cost	Num.Prod.Aircraft	1,000	Study Parameter	500
	O&S Yr	20	”	10 ~ 30
	Cruise Mach	0.82	”	0.74 ~ 0.94

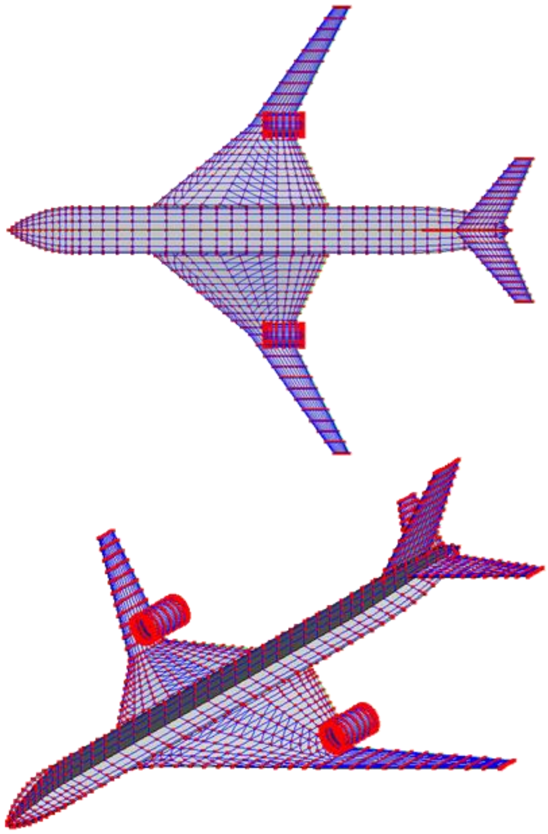

Components	Panel Position		# of Panel
Wing	Chord		33
	Span	Root	6
		Mid	12
		Tip	12
HT	Chord		33
	Span		12
VT	Chord		33
	Span		12
Nacelle	Chord		21
	Span		12
Body	Width		17
	Span	Nose	6
		Cab1	12
		Cab2	12
		Tail	12

Figure 4: VSPAero VLM Tessellation setup of baseline model

$$M_{crit} = \frac{0.87}{cos\theta} - \frac{t/c_{avg}}{cos^2\theta} - \frac{0.1\, C_{L\,Cruise}}{cos^3\theta} - \left(\frac{0.1}{80}\right)^{\frac{1}{3}} \ (\theta = \text{Wing Root Sweep Angle}),\ C_{D\,Rise} = 20(M_{cruise} - M_{crit})^4 \quad (1)$$

DOI: 10.13009/EUCASS2025-016

2.2 Market air-route and earning factor

Range performance of the sized airliner is estimated from the Breguet's range formula; lift-drag ratio is coming from the given cruise condition of wing-loading. Description for the modified formula is given in the author's previous work [6]. Air-route is generated from the list of Major cities in Table 2 and Fig. 5; possible total numbers of the air-route network is 487, combination of the listed cities, however it excludes routes shorter than 400nm for long-haul market analysis. More than that, flight route taking less than 4hrs could be operated twice in a unit period time compared to typical long-haul flight taking about 10hrs.

Earning factor is combination few factors that determines real world flight ticket cost. Popularity of route, number of passenger on board, number of flight per unit period, passenger factor, and distance of flight can be considered, and earning factor formula is assumed as shown in Table 1. The popularity of route is assumed to be proportional to the city index from Global Power City Index Report [11]; total popularity of the route is product of the departure and arrival cities' popularity. The number of passenger on board is passenger number of the sized airliner to investigate impact of the airliner size. The number of flight is usually one but two only when total flight time is less than 4hrs as described above. The passenger factor represents relation between number of passenger and market earning; value lies between zero and one. If the value nears one, market situation is generous for growth and vice versa. Distance between the connected cities is also proportional to earning.

The earning factor is the major driving motivation refining airliner size; aircraft capable of connecting two far and popular cities is recommended to earn more profit for airlines. If market situation were more competitive meaning large airliner taking risk for smaller load factor, the passenger factor nears zero. This leads to the different form of optimized airliner configuration depending on the factor.

Table 2: List of 32 major cities for long range airliner

City	Popularity	Latitude [deg]	Longitude [deg]	Distance [nm] from Seoul
Seoul	1.189	37.5519	126.9918	0
Tokyo	1.367	35.6764	139.65	619.8307
Beijing	1.099	39.9042	116.4074	515.1227
Shanghai	1.133	31.2304	121.4737	467.5449
HongKong	1.068	22.3193	114.1694	1129.517
Taipei	0.963	25.033	121.5654	801.1254
Singapore	1.233	1.3521	103.8198	2522.315
Jarkata	0.756	6.1944	106.8229	2181.329
Sydney	1.115	-33.8688	151.2093	4496.368
NewDelhi	0.627	28.6139	77.209	2531.346
Dubai	1.127	25.2048	55.2708	3663.545
Cairo	0.697	30.0444	31.2357	4582.916
Istanbul	0.997	41.0082	28.9784	4295.734
Moscow	0.991	55.7558	37.6173	3567.789
Rome	1.017	41.8967	12.4822	4843.203
Paris	1.356	48.8566	2.3522	4842.205
Frankfurt	1.073	50.1109	8.6821	4617.538
Munich	1	48.1351	11.582	4616.368
Madrid	1.122	40.4168	3.7038	5183.779
London	1.592	51.5072	-0.1276	4783.686
NewYork	1.505	40.7128	-74.006	5968.605
Chicago	1.058	41.8781	-87.6298	5675.41
Atlanta	1	33.7488	-84.3877	6181.496
Miami	1	25.7617	-80.1918	6708.388
Dallas	1	32.7767	-96.797	5925.985
Seattle	0.976	47.6061	-122.333	4493.918
SanFrancisco	1.066	37.7749	-122.419	4875.364
LosAngeles	1.101	34.0549	-118.243	5175.972

DOI: 10.13009/EUCASS2025-016

MexicoCity	0.817	19.4326	-99.1332	6507.546
SaoPaulo	0.904	-23.5558	-46.6396	9905.358
Buenos Aires	0.864	-34.6037	-58.3816	10492.25
Capetown	0.639	-33.9221	-18.4231	9117.282

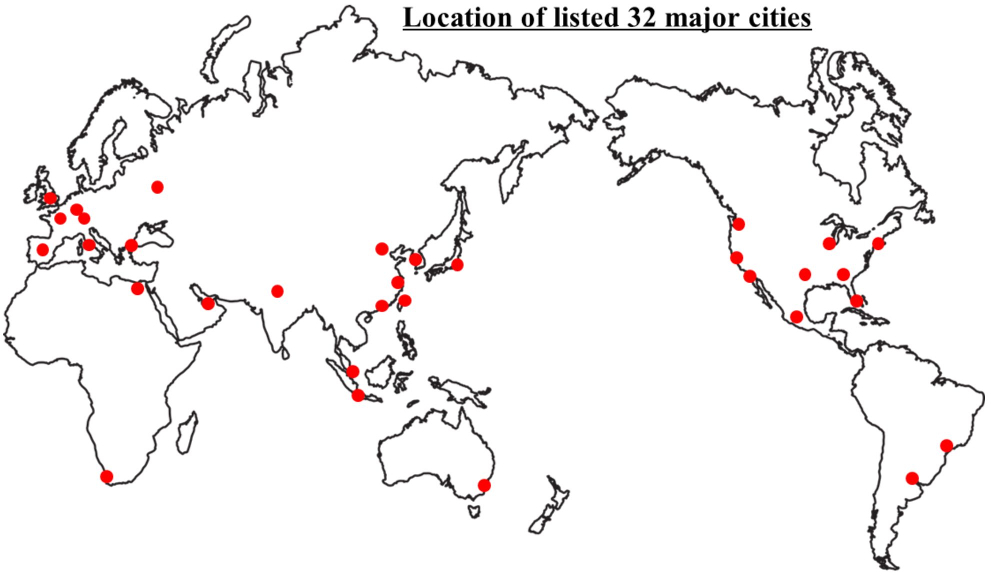

Figure 5: Location of listed 32 major cities

2.3 Cost estimation methodology

Estimating cost of the sized airliner is not easy to be established because it is combination of complex factors from economy, engineering, other major sub-systems like avionics and engine. Because of technological uncertainties related to LH2 implementation on fuel systems, structures, engine, and fuel-cells, built of practical cost model for LH2 airliner is meaningless for current state-of-art. Indeed, the cost model in this paper is only purpose for relative comparison among the sized airliner not to estimate absolute cost of the LH2 airliners. Comparison is relative, and this is caused by size, number of produced airliner, and period of operation and support (O&S).

Author follows modified method of reference [12]; basic rate from the report cannot be applied because of decades of inflation and change of landscape of aerospace industry. Coefficient of initial engineering and tooling cost is adjusted to 120; labour, tooling, material factor is 80. The total number of test aircraft is assumed to be three, and the adjusted cost of aircraft is similar to that of current 787 class airliner for the baseline case with 1,000 produced aircraft. Also, simplification of the model is applied to reduce the number of sub-iteration in whole model. Indeed, iterations in the model is replaced by the simplified and non-iterated equations. These cost estimating terms are related to speed, weight, thrust of engine, and rate of production. As a result, the model could provide research, development, test, and evaluation (RDT&E), and procurement cost.

O&S cost is provided by another reference [13] which cannot be provided by the previous one. Breakdown for several term is applied to estimate aircraft maintenance cost. Most of the terms, similar to that of RDT&E and procurement, are function of each component proportional to the number of seat, aircraft weight, and its specification. Cost for fuel is assumed as maximum fuel load of aircraft which can carry. Sum of the two terms, cost for O&S and fuel, are multiplied by number of operation days and years. More than that total cost is multiplied by square root of procured aircraft; this term represents more produced aircraft has economy of scales for each one. Because of the inflation discussed above, coefficient for cost terms are not fitted to provide correct cost, then author adjusted O&S terms to make ratio between RDT&E + Procurement and O&S about 1:2 for the baseline model. For this case, baseline model is assumed to be procured 1,000 and operated for 20 years.

DOI: 10.13009/EUCASS2025-016

2.4 Post-process using RBF fitting and optimization

The process described above generates sizing data that how much range, efficiency, earning can be achieved by given geometric configuration with sized cost, weight and aerodynamic characteristics. About 15,000 cases were run, and each case were generated via Latin-hypercube method to investigate the studying parameters. Number of input and output parameters are 25 and 39, respectively. Variation of Radial Basis Function (RBF), Elliptic Basis Function (EBF), is selected to generate design space for optimization connecting input and output data. However, because there are many numbers of input and output parameters, final fitted result is not perfect prediction for few parameters. Post-process of Isight SW is used for EBF, and number of sub-iteration is 200. The error of fitted data is evaluated via Root Mean Square (RMS) and R-Squared; acceptable value for the RMS and R-Squared are 0.2 and 0.9, respectively. Most of the parameters passed the criteria however one of the operation efficiency parameter, cruise fuel usage per flying distance per number of passenger, shows lower R-Squared value, 0.84. Indeed, author excludes this parameter during the optimization process. All of parameters satisfies RMS criteria while RMS of the parameters does not exceed 0.1. RMS value of the cruise fuel usage per flying distance per number of passenger is 0.06 which is higher than average RMS value but not highest one.

Optimization was conducted using combination of two methods, NSGA-II [14] and NLPQLP [15]. In author's computing environment, Ryzen 5 5600X 6 core 3.7Ghz CPU and 32Gb RAM, finalizing optimized configuration with generic algorithm takes too much time to achieve satisfying result. Indeed, in order to avoid the gradient method's dependency on initial condition and generic algorithm's resource intensive characteristics, author estimate the initial solution parameter via NSGA-II with smaller number of sets and generation. Then, NLPQLP is applied to find the final optimal parameter values; iteration number for the gradient method is not specifically limited. It is terminated when the configuration design is saturated. Specification for the optimization condition, boundary limit, objective parameters, and their weighting and scale factor, are discussed in the following result section.

3. Analysis and Optimization Result

From the numerous design parameters, resulted performance, and their indexes, composition of parameters for finding right criteria, is not easy task. Additional following up study is required to investigate interpretation and optimization in more depth. Initial attempt of this study focuses on the characteristics of baseline configuration and its sensitivity analysis, and optimizes configuration based on the market situation with relatively simple objective condition.

3.1 Evaluation of baseline configuration

First of all, before optimization process begins, boundary condition for the optimal design should be set. Because basic configuration of the semi-BWB is different from the conventional tube-and-wing, rule of thumb from the conventional one cannot be used. In order to establish the guideline, aerodynamic evaluation of the baseline model for the two conditions, cruise and approach, are conducted. The cruise condition is AoA 3deg at Mach 0.84, and corresponding C_L is 0.27, baseline reference wing loading condition at 37kft altitude. The approach condition without ground effect is AoA 5deg at Mach 0.22 (147kts at sea level), and corresponding C_L is 0.85. Because of its low wing loading, simple deflection flap is only considered in this study; deflection angles of flap are 60, 40, and 20 deg from wing root to tip segment. Contours for the two condition shown in Fig. 6 represent Cp is in the reasonable ranges. Initial coefficient values for estimation of thrust-to-weight (T/W) and wing loading (W/S) are provided from the two conditions, and resulted chart for sizing design space is shown in Fig. 7. Considered performance conditions are stall speed (Vstall) at sea level (110kts), maximum speed at 30kft (Mach 0.9), takeoff field length (8,000ft), maximum rate of climb (ROC, 3,000fpm), maximum ceiling altitude (40kft), sustained turn (2-g) and instantaneous turn (2.5-g) condition at sea level. Appropriate boundary for T/W and W/S are > 0.24 and < 62lb/ft^2 respectively, and this condition is used for further optimization process.

The baseline configuration results L/D = 16 at its cruise condition, Mach 0.84 at 37kft altitude with full payload and half of fuel. As described above, maximum number of passenger on board is 290; empty weight, fuel weight, payload, and maximum takeoff weight are 81, 25.6, 53, and 161t, respectively. Resulted maximum range is 4,480nm (8,300km) which satisfy 197 routes and is little bit shorter than generic long-haul airliners. Total earning of operation assuming 1 as passenger factor is 189,779; 963 is average earning per achievable route. 0.0569 earning per fuel 1kg usage and 0.019658 kg fuel per 1 pax per 1nm cruise are reported. Corrected RDT&E and procurement cost of the configuration, 20yrs of operation with 1,000 procurement and three test aircraft, is 3.2Bil.USD, 319.5Mil USD per aircraft while 303.3Mil.USD is estimated for RDT&E phase only. Total life cycle cost including RDT&E, procurement, and O&S is 596Bil.USD, 596.5Mil.USD per aircraft, and 29.8Mil.USD per aircraft per yr.

DOI: 10.13009/EUCASS2025-016

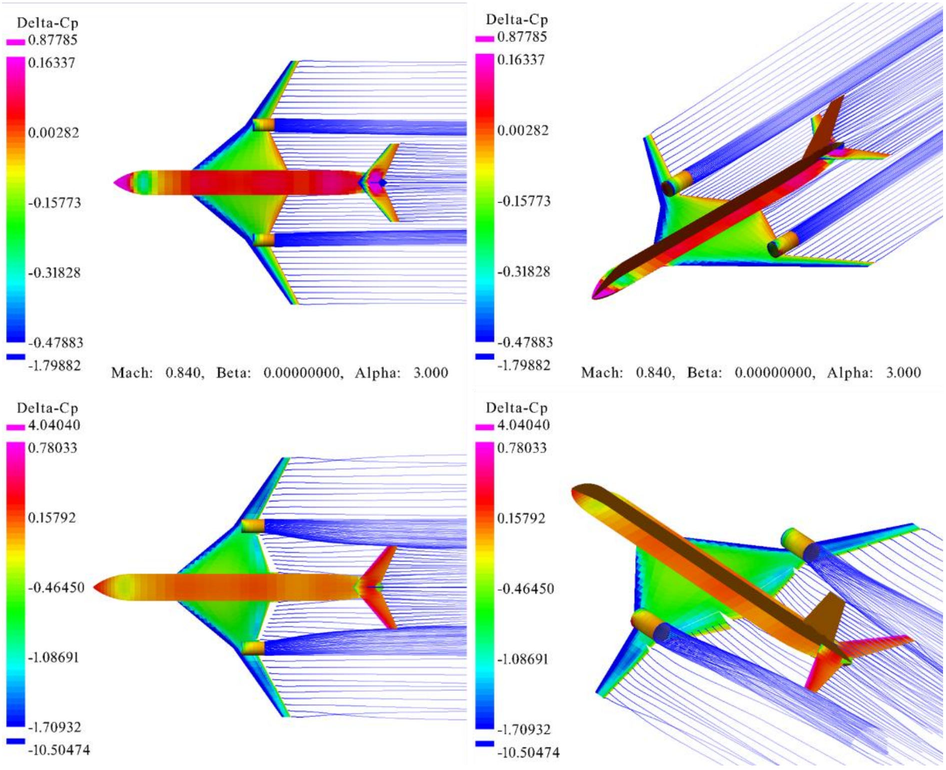

Figure 6: Distribution of Cp for cruise condition: C_L 0.27, AoA 3deg, M0.84 (upper row), and landing condition: C_L 0.85, AoA 5deg, M0.22 with 60/40/20 flap deflection from root to tip (147kts at sea level) (lower row)

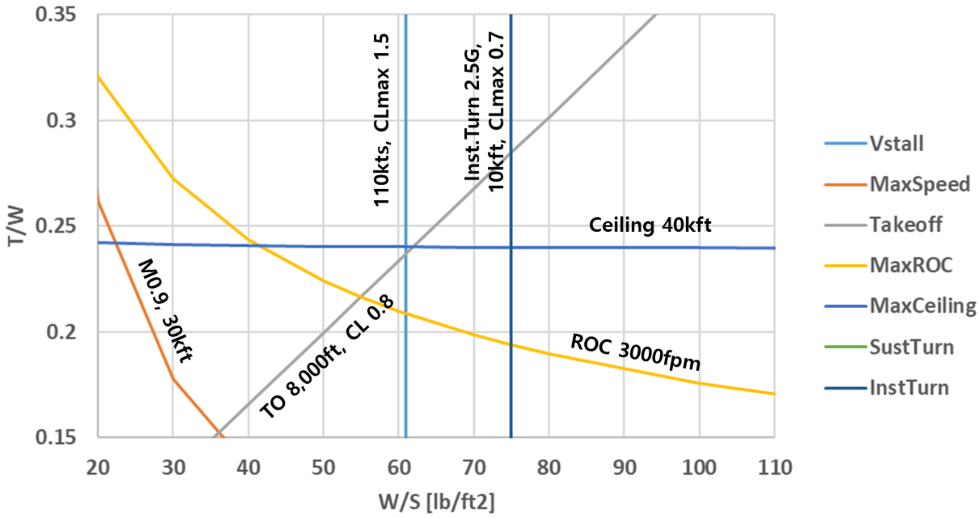

Figure 7: Sizing requirement guideline for thrust-to-weight (T/W) and wing loading (W/S); it is shown that the resulted condition of optimal design should be W/S < 62lb/ft^2 and T/W > 0.24 to achieve desired performance

3.2 Sensitivity analysis

Without configuration changes, effect of TSFC, cruise speed, hybridization of propulsion system and efficiency of fuel cell can be investigated. These affect cruise performance, system weight, and resulted earning performance in operation area. Basically, +-10 percent difference from baseline value is given while hybridization has specific targeted value to find impact of system electrification as shown in Table 3. 1% increase of TSFC, consuming more fuel for

DOI: 10.13009/EUCASS2025-016

thrust, decreases the maximum range as expected, and total earning and number of achievable route is decreased -2.6% and -1.7%, respectively. This trend is more deeply investigated and shown in Fig. 8; overall relation among range, number of course, and earning is logistic curve because of size limit of Earth. As the range become enough to cover the most of the possible route, increase of number of route and earning cannot be significant. Interestingly, there is a slight difference for most efficient range between the number of course and earning. The best range vs number of course point is 6,915nm (12,807km) while the range vs earning is 7,469nm (13,833km). Because longer range route could earn more than the shorter one, optimal point of range is shifted for longer one in case of earning. The inferred optimal range is similar to that of current long range airliners like 330, 350, 777, and 787s. Increase of cruise speed reducing cruise C_L and L/D slightly increases the earning and number of achievable route however impact of the parameter is not significant than the other parameters we discussed here.

Hybridization of the propulsion system adding fuel cell to generate electricity changes overall system weight and performance. Percentage of hybridization means proportion of fuel cell generated electricity compared to total generated power; 50% means maximum electric power from the fuel cell is equal to that of direct hydrogen combustion engine. Generally, as described above, addition of fuel cell makes aircraft heavy however, fuel-cell-TSFC is more efficient than direct combustion. This tendency is also shown for the baseline configuration in Table 3. Pros and cons of fuel-cell is compensated and net effect of hybridization on the performance is not significant; only one percent of range increase is reported for 30% of hybridization. Reduction of the emission from the hybridization is expected to be effective for more than the 30% because cruise phase generating most of the direct combustion emission usually requires 20~30% of maximum power at sea level. Also this trend is based on the fuel cell efficiency is 0.55 level of the best solid oxide fuel cell (SOFC). If efficiency of fuel cell falls to 0.3, range is decreased -5.6% by 30% of hybridization. This performance degradation leads to -12% of total earning and -6.3% of earning per unit fuel usage.

Issue for the hybridization and fuel cell efficiency is added weight; most of the added one is expensive fuel cell, battery, and thermal management system. Scalability of the huge power fuel cell system generating MW level is unproven, and following expense is unpredictable at current state of art. Another issue for the hybridization is concern of aircraft wing loading change via added weight; cases of the Table 3 are already over the design boundary of wing loading. The change of wing loading affects overall design of wing; design of flap for the field performance and transonic drag rise in cruise condition should be considered. Specifically, thickened wing root is prone to drag rise in transonic and high sectional lift coefficient. If we could expand our design boundary for T/W and W/S as 0.24 and 80, optimal hybridization point can be explored by design space as shown in Fig. 9. Change of the maximum engine thrust and hybridization could achieve longer range than the baseline via decreasing T/W and increasing W/S.

Table 3: Performance and operation efficiency sensitivity via non-configuration parameters

Result	**Baseline**	**TSFC 1%**	**Cruise Speed 1%**	**Hybridization (cell efficiency = 0.55)**			**Fuel cell efficiency (Hybridization = 30%) (%) is Δ from eff. 0.55**		
				10%	**30%**	**50%**	**0.3**	**0.45**	**0.6**
Earning per fuel [1/kg]	0.0569	-0.98%	0.05%	0.057 (0.84%)	0.0576 (1.3%)	0.0567 (-0.2%)	0.054 (-6.3%)	0.057 (-1.1%)	0.058 (0.63%)
Earning per course	963.3	-1.13%	0.3%	967 (0.4%)	979 (1.6%)	965 (-0.15%)	930 (-5.1%)	967 (-1.2%)	984 (0.5%)
Total Earning	189,779	-2.6%	0.5%	192,179 (1.3%)	197,071 (3.8%)	187,572 (-1.2%)	174,540 (-12%)	191,440 (-1.8%)	199,640 (1.3%)
Cruise C_L	0.26	-	-1.92%	0.27 (3.8%)	0.31 (19%)	0.36 (38%)	0.34 (11%)	0.32 (3.8%)	0.31 (0%)
Achievable Route #	197	-1.7%	0.15%	200 (1.4%)	202 (2.8%)	196 (-0.7%)	189 (-6.9%)	198 (-2.1%)	204 (0.7%)
Fuel usage per distance per pax [kg/nm/#]	0.0197	0.99%	-0.05%	0.019 (-0.86%)	0.019 (-0.86%)	0.019 (-0.86%)	0.020 (4.3%)	0.019 (0%)	0.023 (0%)
Cruise L/D	16	-	-0.81%	16 (3%)	17 (8.2%)	18 (12.6%)	18 (3.0%)	17 (0.74%)	17 (0%)
Cruise Range [nm]	4480	-0.9%	0.05%	4,517 (0.8%)	4,525 (1%)	4,460 (-0.44%)	4,273 (-5.6%)	4,474 (-1.1%)	4,561 (0.82%)

DOI: 10.13009/EUCASS2025-016

Hybrid system weight [kg]	0	-	-	10,038	34,708	65,463	48,874	37,656	32,743
Hybrid req. power [MW]	0	-	-	11	40	75	42	37	39
W/S [lb/ft2]	62	-	-	66	75	86	81	76	74

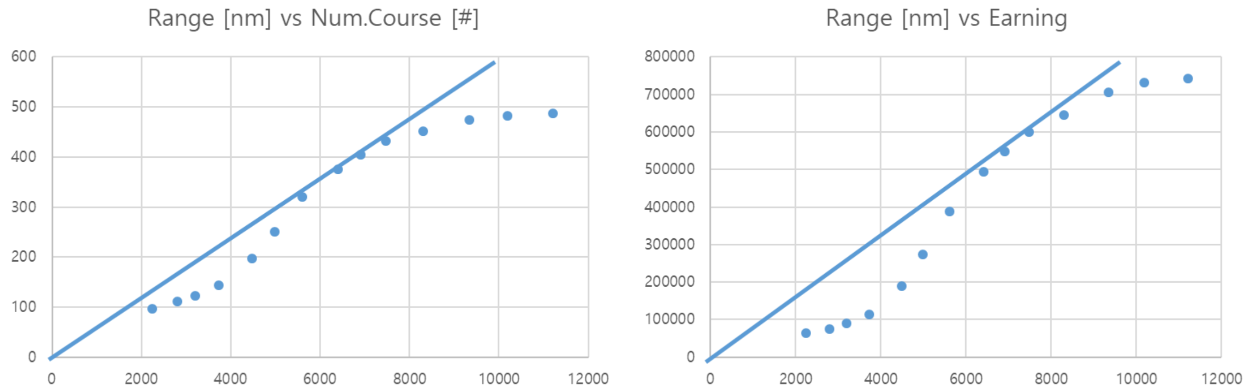

Figure 8: Trend among airliner range, number of achievable route, and operation earning

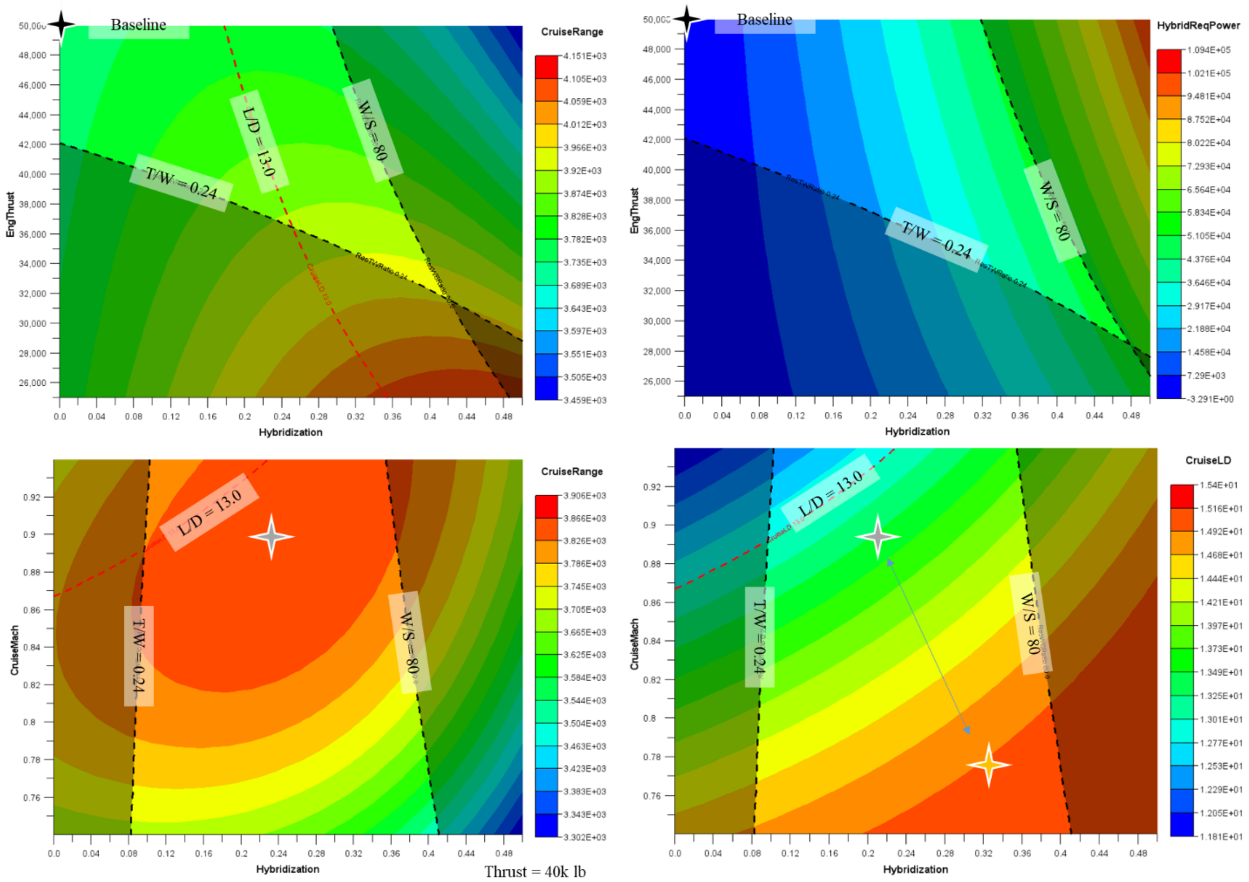

Figure 9: Design space contour via change of propulsion system

DOI: 10.13009/EUCASS2025-016

3.2 Configuration optimization

Multi-disciplinary optimization (MDO) for those kinds of problem should be careful for objective setup because inappropriate scale or weight factor leads to unbalanced approach for the configuration. This initial study uses relatively simple combination and focuses effect of market situation on the optimal configuration. As described above, T/W and W/S are bounded at 0.24 and 62 lb/ft2 while hybridization is kept as zero for simplicity in this case. Major objectives are maximization of earning per route and earning per unit fuel usage which represents operation efficiency of the airlines. Environment condition affecting market earning is defined by passenger factor, and it can be shown that optimal configuration is depending on the market situation. Market situation is given as four cases; Ideal (factor = 1), Good (factor = 0.9), Generous (factor = 0.75), and Hard (factor = 0.3) are defined, and proper scale factor is set weighting of two objectives in similar value. Optimization process for the given boundary conditions and objectives follows the process described in the section 2.4.

Overall comparison for the optimized configuration is shown in Table 4 and Fig. 10. The optimized configuration has similar wing loading, cruise C_L, of the baseline while they could go further range and more routes than the baseline due to the optimization effort. However, specific performance of the optimized ones is very different among them. When the market is in the ideal condition, optimal design evolved to have longer range and load more passengers. It reaches the maximum fuselage size given in the study which could load 405 passengers on board. Maximum range of the ideal one is also the longest among the optimized designs which has 7,047nm maximum range and 416 routes in the air-routes network. The range performance is similar to optimal point of the range vs earning or achievable routes. As the market situation is far from ideal condition, optimized design become smaller and load less passenger than the ideal one. Fuel load on the airliner is concentrated on the fuselage for the whole optimal designs; root trailing edge fillet become larger than the usual designs. This trend is little bit reversed at the hard market condition. Although hard market loads smallest number passenger on board, range is slightly longer than the generous one, and has different style of wing planform than the other designs.

Table 4: Operation efficiency and performance of optimized configuration

Result	Baseline	Optimized Configuration			
		Ideal	Good	Generous	Hard
		Pax Factor 1	0.9	0.75	0.3
Scale factor 1	(Earn per course)	1,000	500	200	10
Scale factor 2	(Earn per fuel)	0.05	0.02	0.01	0.001
Achievable Route #	197	416	360	302	340
Fuel usage per distance per pax	0.0197 [kg/nm/#]	0.0189	0.0183	0.021	0.022
Pax [#]	290	405	373	285	253
Cruise L/D	16	20	18	16	17
Cruise Range [nm]	4,480	7,047	6,092	5,372	5,849
MTOW [t]	161	270	223	176	166
Empty weight [t]	135	216	181	144	133
Fuel weight [t]	25.6	54	42	32.3	32.6
Wing AR	6	4.3	4.1	4.1	6.1
Wing Area [m^2]	527.4	897	734	580	580
Wing Span [m]	56.4	62.2	54.6	48	59
Max. Thrust per engine [lbf]	50,000	66,740	56,810	44,530	42,300

DOI: 10.13009/EUCASS2025-016

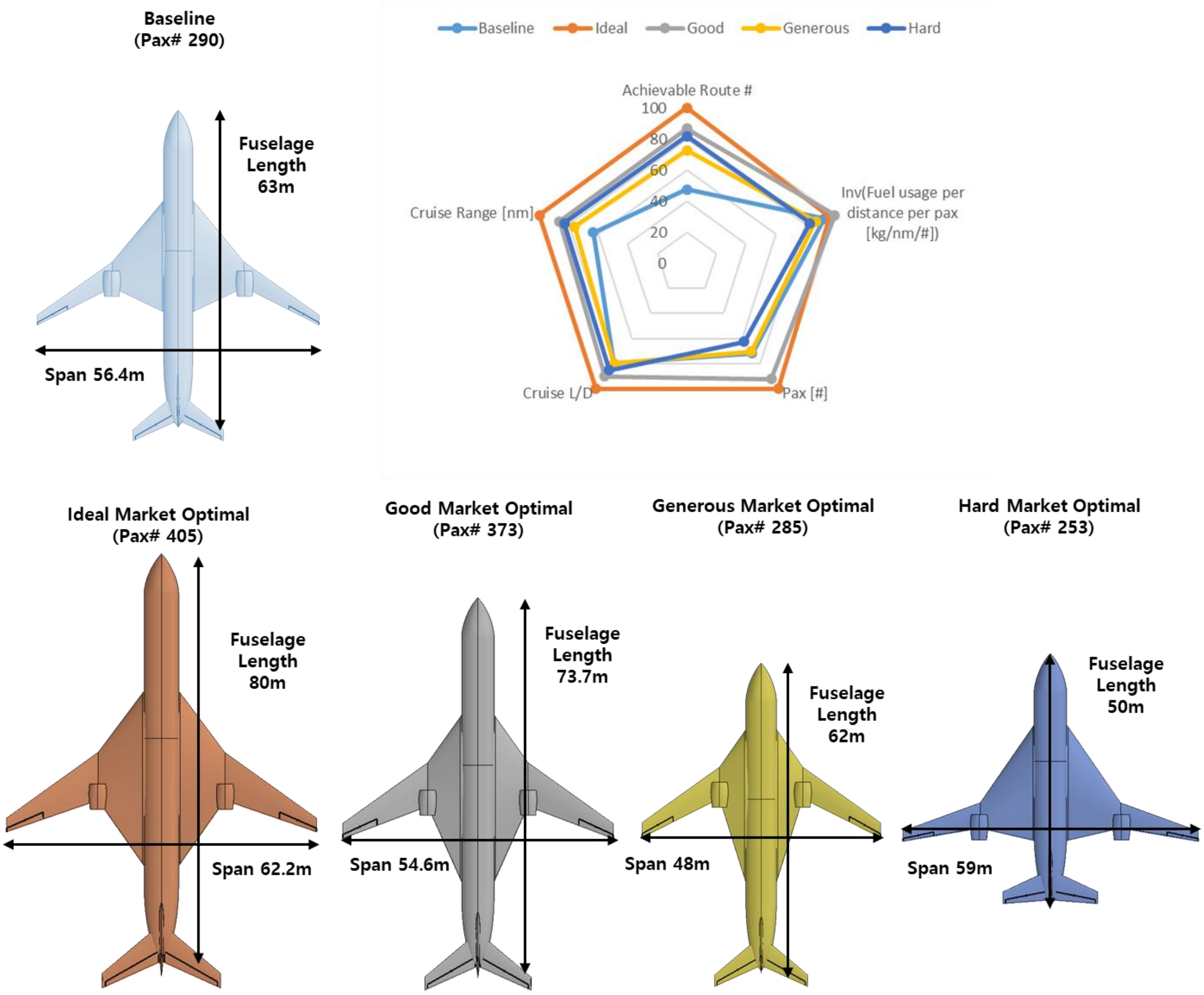

Figure 10: Comparison of optimized configurations

4. Conclusion

This paper continues and expands author’s previous work for the design of LH2 long range airliner; functionality of framework including design and evaluation parameters are proliferated. It helps to describe the aircraft sizing with better accuracy and tendency changes. Operation efficiencies are simultaneously calculated, and this represents that sizing should be not only result of given performance condition but also market adaptation of airlines. Recommended range and passenger carrying performance for the optimal airliner configuration is changed and tendency is shown in the initial attempt of optimization.

Because many numbers of objective are considered in the study, sophisticated combination is yet attempted to optimize the configuration. Future study would investigate the cost boundary, market performance, and combination of the concerned parameters to make better and robust result. More concerned parameter is optimization of aeroelasticity perspective for wing box structure which is only roughly estimated from the sizing equations. Later work would add aeroelasticity module to give better estimation of wing box configuration. At last, re-visit of LH2 cargo aircraft sizing for both military and civil is planned using the updated features of the current and near future studies.

DOI: 10.13009/EUCASS2025-016

References

[1] Zubi, G., Kuhn, M., Makridis, S., and Coutinho, S., Aviation sector decarbonization within the hydrogen economy – A UAE case study,
: In future 2050 – realistically aircraft fuel option, 2070 – become major fuel if it gains momentum
[2] Wood, N. J. Hales, M. O. Joynt, M. Devendran, S. and Taylor, S. 2024. Scalability of Hydrogen Fuel Cell Aircraft. In: *AIAA Aviation Forum and ASCEND 2024*. AIAA2024-3659. 1-12.
[3] Guynn, M. D. Freeh, J. E. and Olsen, E. D. Evaluation of a Hydrogen Fuel Cell Powered Blended-Wing-Body Aircraft Concept for Reduced Noise and Emissions. NASA/TM-2004-212989.
[4] Karpuk, S. Ma, Y. and Elham, A. Design Investigation of Potential Long-Range Hydrogen Combustion blended Wing Body Aircraft with Future Technologies. Aerospace 2023. 10. 566.
[5] https://www.jetzero.aero/ (Accessed 2025.02.21)
[6] Yoon, J. S. 2024. Initial Design of Semi-BWB Type Hydrogen Fueled Transport Based on Operational Performance. In: *AIAA AVIATION FORUM AND ASCEND 2024*. AIAA2024-3662. 1-13.
[7] Raymer, D. P. 2024. Aircraft Design: A Conceptual Approach. AIAA Educations Series.
[8] Brewer, G. D. 1991. Hydrogen Aircraft Technology. 1st ed. CRC Press. Boca Raton.
[9] Chinnici, G. 2024. Conceptual Design of a Commercial airliner powered by hybrid-hydrogen architecture. MS Thesis. Politecnico di Torino.
[10] Patel, S. Ahuja, J. Ragauss, E. Gladin, J. and Mavris, D, N. 2024. Development of a Blended Wing Body Aircraft with Hydrogen-Electric Hybrid Distributed Propulsion. In: *AIAA SciTech 2024 Forum*. AIAA2024-0282. 1-20.
[11] The Mori Memorial Foundation's Institute for Urban Strategies. 2022. Global Power City Index Report.
[12] Boren, Jr. H. E. 1967. DAPCA: A Computer Program for Determining Aircraft Development and Production Cost. The RAND Cooperation. RM-5221-PR.
[13] Maddalon, D. V. 1978. Estimating Airline Operating Costs. CTOL Transport Technol. Conf. NASA-TM-78694.
[14] Deb, K., Pratap, A. Agarwal, S. and Meyarivan, T. 2002. A fast and elitist multi-objective genetic algorithm: NSGA-II. *IEEE Transactions on Evolutionary Computation*, vol. 6, no. 2, pp. 182-197.
[15] Schittkowski, K. NLPQLP: A Fortran Implementation of a Sequential Quadratic Programming Algorithm with Distributed and Non-Monotone Line Search. User's Guide. Version 4.2.